JOURNAL OF MATERIALS SCIENCE 4 (1969) 653–657

The Cyclic Stress Behaviour of a 355 Stainless Steel 2024-T8 Aluminium Alloy

A. VARSCHAVSKY, P. TAMAYO
Institute of Research and Testing Materials, University of Chile

Received 25 November 1968, and in revised form 28 April 1969

The push-pull fatigue behaviour of a 355 stainless steel 2024-T8 aluminium alloy composite, has been studied at constant stress. The S–N curve shows a fatigue strength of 20 kg/mm². Microhardness measurements reveal that little fatigue hardening takes place within the matrix; also, hardness numbers are similar in fatigued specimens, irrespective of the applied stress amplitude.

The increase in damping capacity for increasing stress amplitudes, is attributed to increased delamination at the fibre-matrix interface, in the early fatigue stages. This result is also confirmed by optical microscopy. It is inferred that the sequence of failure weakness in the composite is: fibre-matrix interface, matrix and, finally, fibres.

A fatigue strength/tensile strength ratio of 0.16 for this material is noticeably low, but fatigue properties of the composite can be improved by enhancing the fibre-matrix bonding.

1. Introduction

Metal/matrix fibre composites have very good properties, including their strength to weight ratio and stiffness values. The behaviour, under steady stress, of a 355 stainless steel 2024–T8 aluminium alloy composite has been studied, together with its strain hardening and stiffness characteristics [1].

The object of the present work was to study the cyclic stress behaviour of the above material. This included the experimental measurement of cyclic strain hardening in the matrix.

Another important objective of this work was to find the sources of weakness in the composite, and the sequence which led to final failure.

2. Experimental Procedure

2.1. Material and Preparation of Samples

Experiments were performed with a 2024–T8 aluminium/355 stainless steel composite plate, supplied in 0.25 in. thickness by Harvey Aluminium of Torrance, California, USA. The stainless steel wires, of 0.009 in. diameter, were arranged as a continuous unidirectional reinforcement, representing approximately 25% of the total volume. Fabrication of the composite involved assembly of aluminium sheet and the stainless steel wires in alternate layers. This assembly was hot pressed at 468° C for 30 min to promote diffusion bonding, and then air cooled. The composite was next heat-treated at 488° C, hot water quenched, cold rolled 1% for flattening, and then aged at 191° C for 10 h. Rectangular-section specimens, 0.2 in. wide, 0.24 in. thick, with a gauge length of 1.2 in. were spark machined in a servomet spark-cutter machine. In each fatigue specimen section there were approximately 85 to 90 wires. After the spark-cutting process, samples were electropolished in a solution of 33.33% perchloric acid and 66.66% acetic anhydride at 0° C for 5 min, under a voltage of 24 V [2]. This reagent was suitable for polishing the wires and the matrix.

2.2. Phenomenological Behaviour

Push-pull fatigue tests were carried out in an Amsler Vibrophore machine, at constant stress. Vickers microhardness tests were made on virgin and fatigued specimens, using a Leitz Durimeter Tester with a 100 g load. This load was chosen in order to average the grain orientation effects in the matrix. Damping measurements were per-

formed during the fatigue process using a special drum camera [3]. The damping capacity was computed from the relation:

$$\delta = \frac{1}{n} \log_e \frac{A_0}{A_n}$$

A_0 is the amplitude of the first vibration.
A_n is the amplitude of the $(n + 1)$ vibration.

2.3. Microstructure

Longitudinal and transverse cross-sections of the fatigue specimens were examined by optical microscopy after testing. The sections were etched with the reagent mentioned in 1.1, at 0° C, with a voltage of 18 V.

3. Results

3.1. Phenomenological Behaviour

The S–N curve shown in fig. 1, would suggest that the material tested had a fatigue limit of approximately 20 kg/mm², reached after 10^7 cycles.

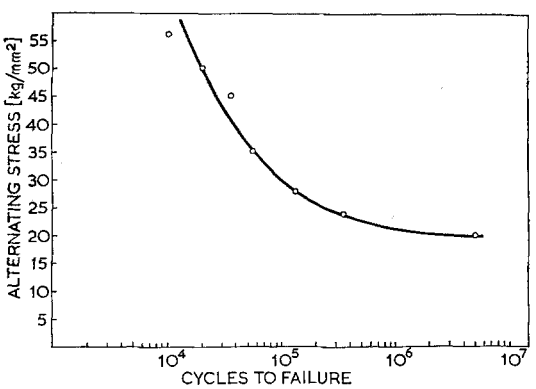

Figure 1 S–N curve in the direct stress push-pull mode.

Decay recordings for two stress amplitudes are shown in fig. 2. Damping capacity was computed for specimens subjected to different stress amplitudes, after the transient stage of cyclic deformation had disappeared. Damping reached constant values that covered a long cycle range, as shown in fig. 3. The higher the stress amplitude, the higher was the damping capacity. Since the vibrophore is a high frequency machine, it was not possible to compute damping values in the early stages of the fatigue test by the procedure described in [3]. The results of fig. 3 are plotted in terms of stress amplitude in fig. 4. In this figure, it can be observed that at low fatigue stresses, damping capacity increases

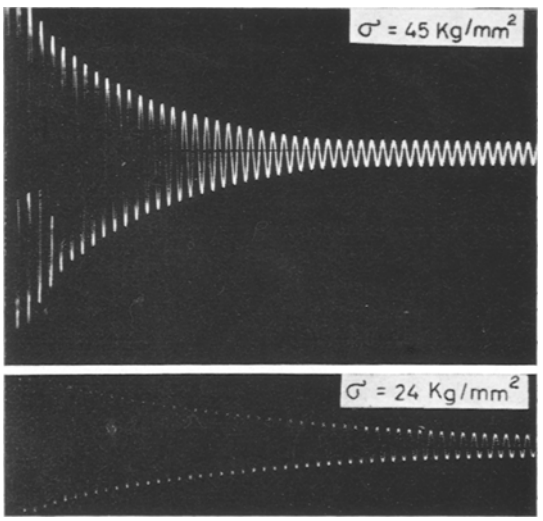

Figure 2 Damping records for two specimens subjected to different stress amplitudes.

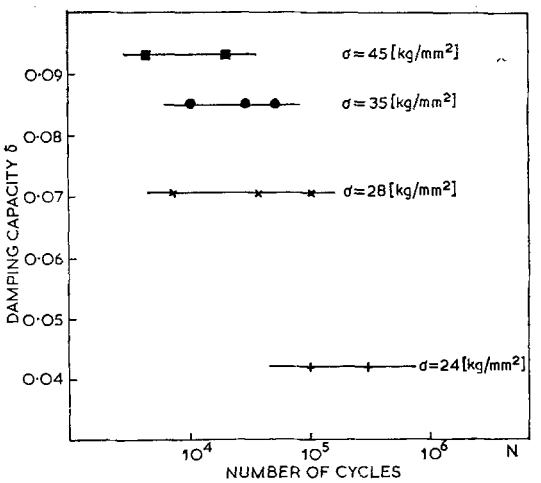

Figure 3 Damping capacity versus number of cycles of fatigue, for different stress amplitudes.

rapidly with small increases in stress, but, at high stresses the increment becomes less.

The Vickers microhardness along the matrix, between pairs of equally spaced fibres, is plotted in fig. 5 for fatigued samples. This figure shows that the dispersion in microhardness numbers is not higher than 13.5%, about an average value of 148, irrespective of the applied stress amplitude. Furthermore, no appreciable differences in hardness numbers were observed in regions near the fibres and midway between them.

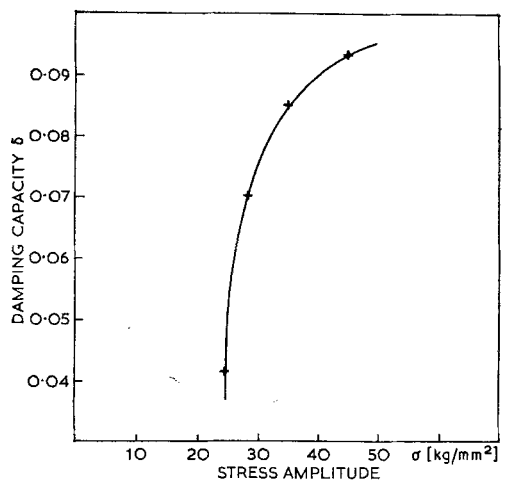

Figure 4 Damping capacity as a function of stress amplitude.

In virgin specimens (same figure), the average microhardness is 136, with a dispersion of 16.2%. Hardness scatter bands, for virgin and fatigued specimens, overlap by almost 50%.

3.2. Microstructural Observations

By increasing the stress amplitude, the amount of cracking which concentrates principally in the fibre-matrix interface, increases. The micrograph of fig. 6 illustrates unbonding of a fibre-matrix interface; the section is parallel to the fibre axis. It is generally observed that, when further unbonding of fibre-matrix interfaces ceases, cracks then propagate through the matrix and finally through the steel wires. The spread of a microcrack from an interface into the matrix is shown in fig. 7.

Before a crack propagates to another fibre, it runs along matrix-interface paths, as in fig. 8. Aluminium–aluminium diffusion bonds located almost perpendicular to the fracture direction, are revealed in this figure (see arrows D) and have never been found disrupted.

Crack propagation was both inter- and transcrystalline through the matrix, and both types of cracks were observed irrespective of the applied stress amplitude. Fig. 9 illustrates a crack which propagated perpendicular to the fibre axis, penetrating into the grains.

4. Discussion of Results

It has already been established from microhardness numbers, that little fatigue hardening takes place in the matrix. This result is very similar to the one obtained in steady state stress

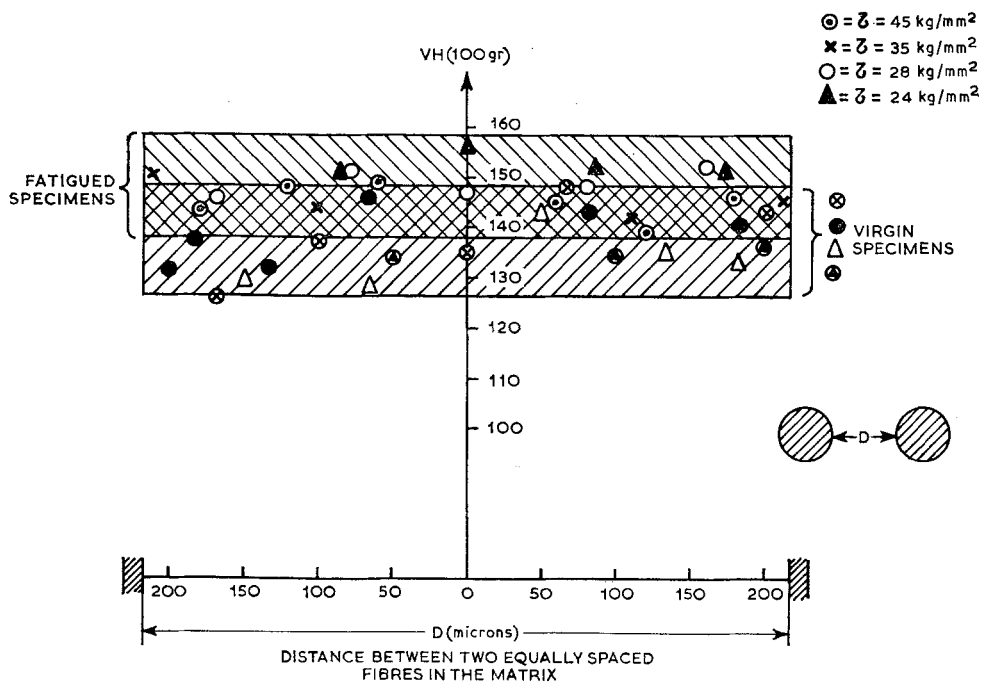

Figure 5 Vickers microhardness for virgin and fatigued samples versus stress amplitude. Microhardness numbers were taken in different specimens between pairs of equally spaced fibres.

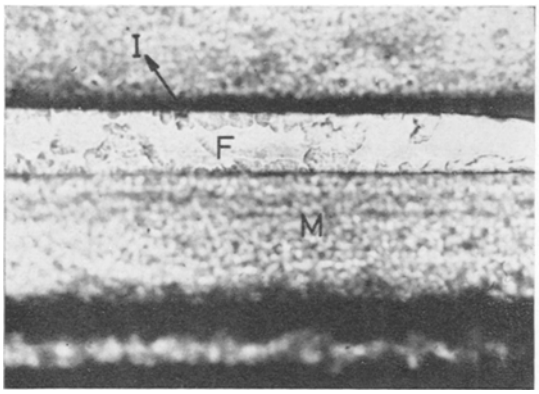

Figure 6 Delaminated interface at I in a fatigued sample cycled at $\sigma = 28$ kg/mm^2 after 115 000 cycles: F, fibres; M, matrix (× 64).

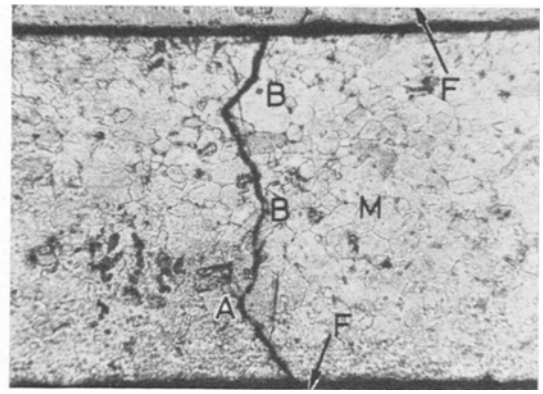

Figure 9 Crack propagation through the matrix in a sample stressed at $\sigma = 20$ kg/mm^2 after 5 000 000 cycles: F fibres; M, matrix. Crack propagation is intercrystalline at A and transcrystalline at B (×64).

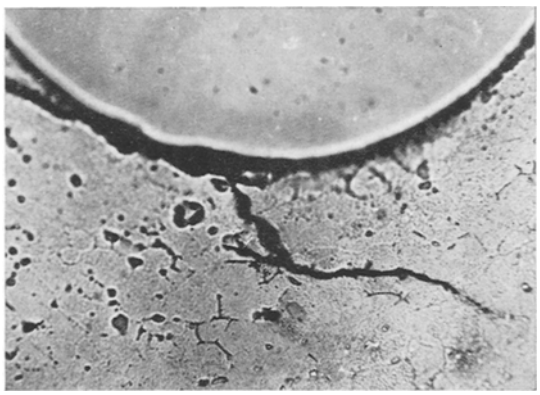

Figure 7 Microcrack growing from a debonded fibre-matrix interface in a sample stressed at an amplitude $\sigma = 35$ kg/mm^2 after failure at 55 000 cycles (× 318).

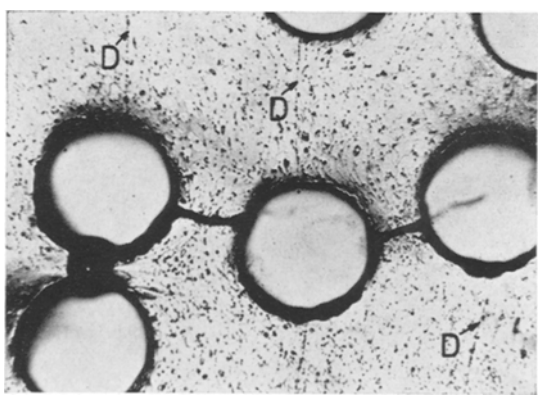

Figure 8 Microcrack propagation along an interface-matrix-interface path, in a sample fatigued at $\sigma = 50$ kg/mm^2 after 20 000 cycles. Aluminium–aluminium diffusion bonds (D) run almost perpendicular to the crack (×64).

tests [1]. An explanation of this phenomenon could be that the restraining effect of the fibres [1, 4], contributes to a triaxial state of stress in the matrix. The small difference in microhardness among specimens fatigued at different stress amplitudes, is additional proof that there has been little deformation in the matrix, since it would be expected that the higher the stress amplitude, the higher would be the fatigue hardening [5].

The foregoing results predict that damping capacity values should be similar in high and low cycling fatigue experiments, but, actually, these values differed by 68% in specimens with lives between 10^4 and 10^7 cycles. This effect cannot be attributed to internal friction depending upon stress amplitude, which is invariably associated with unpinning and movement of dislocations [6], leading to plastic deformation in the matrix. Furthermore, internal friction due to deformation of the fibres themselves, must be negligible, since, in the range of stress used, they are behaving elastically [1]. This would not be so if considerable cracking had occurred in the matrix.

The source of the internal friction must be the debonding of the fibre-matrix interface. This prevents shear strain transfer, which leads to a damping effect from the loss of continuity of the solid.

Since damping capacity remains constant during the steady state cyclic period, local debonding should occur in the early transient stage of the test, being more accentuated at higher stresses. Local debonding does not necessarily accelerate failure, but it must be

regarded as the first step in the sequence that leads to it.

The tendency for damping to approach a constant value at high amplitudes, indicates, from the foregoing considerations, that a similar amount of delamination of fibre-matrix interfaces takes place at these stress levels. On the other hand, at low amplitudes, this effect is very sensitive to the applied stress.

From the debonded interfaces, microcracks grow into the matrix and afterwards into the fibres, as revealed microscopically.

The presence of transcrystalline cracks in the matrix is typical of fatigue at low stress levels [7]. These facts are in accordance with the small amount of cyclic strain hardening experienced by the matrix. After considerable cracking of the matrix, breakage of fibres will occur. This is attributed to the reduction of the effective cross sectional area of the specimens.

At low or high fatigue stress no different fatigue mechanisms seem to be distinguishable, but different stress levels lead to dissimilar degrees of delamination. According to this the probability of cracks growing into the matrix should vary.

One of the possible causes of debonding is the presence of $FeAl_3$ and $CuAl_2$ compounds, formed in the fibre-matrix interface during the manufacturing process [8]. These intermetallic compounds give poor shear transfer, and because of their brittle nature they break and cause delamination.

Finally, the mechanical strength of the composite is compared with that of the constituent materials in table I. (Mechanical tests on the steel were carried out on standard size specimens rather than wire.)

TABLE I

	Steel	Al Alloy	Composite
Tensile strength (kg/mm²)	70.6	51	122
Strength/specific weight (mm)	8.83×10^6	18.4×10^6	30.6×10^6
Fatigue strength (kg/mm²)	37.3	12.8	18
Endurance ratio	0.53	0.25	0.16
Fatigue strength/ specific weight (mm)	4.66×10^6	4.26×10^6	4.59×10^6

The above data shows a good performance of the composite for steady stress tests but it has no advantages as regards fatigue endurance ratio or specific fatigue strength.

5. Conclusions

(i) 355 stainless steel 2024–T8 aluminium alloy composite has a fatigue strength of 20 kg/mm² under push-pull fatigue tests.
(ii) Little fatigue hardening is produced in the matrix, irrespective of the applied stress amplitude.
(iii) The hardness is similar in the matrix away from and in the neighbourhood of fibres.
(iv) The sequence of failure in the system is: (*a*) fibre-matrix interface; (*b*) matrix; (*c*) fibres.
(v) The endurance ratio is lower for the composite than for the constituent materials; specific fatigue strength values are similar.
(vi) The fatigue properties of the composite might be increased by improving the fibre-matrix bond.

Acknowledgements

The authors wish to thank Dr R. C. Jones for supplying the composite, and Dr G. Joseph for the facilities given at the Metals Center of the University of Chile

References

1. R. C. JONES, "Deformation of wire reinforced metal matrix composites" (ASTM Symposium on metal matrix composites, Boston, Mass, June 1967).
2. P. A. JACQUET, A. R. WEIL, and I. CALVET, *Acad. Sci. France* **247** (1958) 1001.
3. J. ALFRED AMSLER & CO, Schaffhausen (Switzerland), Description No. 205.
4. H. M. BURTE, P. R. BONANO, and J. A. HERZOG, Metal matrix composite material, in "Orientation effects in the mechanical behavior of anisotropic structural materials" ASTM STP 405 *Amer. Soc. Test Mats.* (1966) 59-95.
5. C. F. FELTNER and C. LAIRD, *Acta Met.* **15** (1967) 1621.
6. GRANATO and LUCKE, *J. Appl. Phys.* **27** (1956) 583.
7. J. PORTER and J. C. LEVY, *J. Inst. Metals* **89** (1960) 86.
8. W. DAVIS LE ROY, *Met. Prog.* **91** (1967) 105.